J Solid State Electrochem (2015) 19:543–548
DOI 10.1007/s10008-014-2550-8

ORIGINAL PAPER

# A simple fabrication of Ag-nanowires@$TiO_2$ core-shell nanostructures for the construction of mediator-free biosensor

**Hui Liu · Xiaonan Dong · Congyue Duan · Zhenfeng Zhu**

Received: 28 March 2014 / Revised: 28 May 2014 / Accepted: 21 June 2014 / Published online: 20 September 2014


**Abstract** One-dimensional Ag-nanowires@$TiO_2$ core-shell nanostructures (ANTNs) have been synthesized via a simple solvent thermal method and employed to immobilize hemoglobin (Hb) in order to fabricate a mediator-free biosensor. Immobilized Hb on ANTNs protected by nafion film exhibited good bioactivity, stability, and remarkable electron transfer rate because of its unique core-shell structure and compose. The morphology and structure of the ANTNs were characterized by scanning electron microscopy (SEM) and X-ray diffraction (XRD). Electrochemical measurements revealed that the ANTNs were an immobilization support with biocompatibility for enzymes, affording good enzyme stability and bioactivity. Due to the unique Ag-nanowires@$TiO_2$ core-shell nanostructures, the resulting biosensor displayed good performance for the detection of $H_2O_2$, with both a low detection limit of 1.3 μM and a wide linear range of 4–152 μM, as well as a fast response and excellent long-term stability.

**Keywords** Cyclic voltammetry · Biosensors · Core-shell structure · Nanocomposites

## Introduction

Recently, metal oxide-based semiconductors have attracted much more attention and wide applications in microelectronics, optoelectronics, catalysis, and optical devices because of their superior physical and chemical properties [1–3]. Due to its good biocompatibility, environmentally benign nature, and chemical and thermal stability, $TiO_2$ has become a potential material for immobilization of enzymes [4–6]. As we all know, the morphology and structure will affect the performance of the immobilized enzyme [7]. Nowadays, $TiO_2$ with various morphologies, such as nanowires [8], nanotubes [9, 10], and nanosheet [11, 12], have been applied in developing biosensors. During these forms, $TiO_2$ nanowires have attracted much more attention owing to its unique structure and superior ability in immobilization of enzymes [8]. However, the relatively low direct electron transfer rates of rare $TiO_2$ nanowires still limits the further application in the mediator-free biosensors.

Many modifiers, such as noble metal [13, 14], carbon materials [15–17], etc., have been introduced into $TiO_2$ in order to solve the problem. Noble metal could not only provide a friendly microenvironment to maintain the biocompatibility of immobilized enzymes, but also act as the conducting tunnel to facilitate the electron transfer rates in electron pathway [18–20]. Ag nanoparticles have become important compositions for improving the electron transfer rates of Ag-$TiO_2$ hybrid materials because of its much stronger extinction coefficient of surface plasmon band and synergistically enhanced chemical activities than that of others (such as Au) with the same size [13, 14, 21]. Furthermore, to the best of our knowledge, rare works have reported the Ag-$TiO_2$ hybrid nanomaterials for constructing electrochemical biosensors. Nowadays, the synthesized methods of Ag-$TiO_2$ hybrid materials are mainly about chemical reduction [22], photo deposition [23], and electrochemical reduction [24], whose complex processes need to regulate and control all kinds of parameters accurately. Besides, metal nanoparticles could easily aggregate and migrate from $TiO_2$ when the active metal species only attached on the surface of $TiO_2$ so as to largely limit their wide applications in biosensor and fields.

**Electronic supplementary material** The online version of this article (doi:10.1007/s10008-014-2550-8) contains supplementary material, which is available to authorized users.

H. Liu (✉) · X. Dong · C. Duan · Z. Zhu
School of Materials Science and Engineering, Shaanxi University of Science and Technology, Xi'an 710021, People's Republic of China
e-mail: liuhui@sust.edu.cn

It is worth noting that combining the advantages of Ag and $TiO_2$ and fabricating the Ag@$TiO_2$ heterostructured nanomaterials with Ag cores and $TiO_2$ shells can construct more promising electrochemical biosensors in comparison with Ag or $TiO_2$ nanoparticles. Herein, one-dimensional Ag-nanowires@$TiO_2$ core-shell nanostructures (ANTNs) were synthesized via a simple in situ hydrothermal method and their application to mediator-free biosensors. On the one hand, the rough $TiO_2$ shell that possessed good biocompatibility could adsorb abundant protein in order to improve the immobilization of enzymes. On the other hand, the silver core that existed in the ANTNs could accelerate the electron transfer between $TiO_2$ and hemoglobin. Therefore, all of which could enhance the immobilization of hemoglobin and accelerate electron transfer in the electrochemical reaction so as to improve the property of mediator-free biosensor.

## Experimental

*Preparation of ANTNs and Hb-ANTNs-Nafion/GC-based biosensor* Phosphate buffer solution (PBS; 0.1 M, pH 7.0) was prepared with $NaH_2PO_4$ and $Na_2HPO_4$. All chemicals were analytical grade and used without further purification. In a typical synthesis, 1 g tetrabutyl titanate (TBOT; Beijing Chemical Regent Co., China) was added dropwise into 39 mL ethylene glycol (EG; Tianjin Kermel Chemical Regent Co., Ltd., China) containing desired amounts of $AgNO_3$ (Guanghua Chemical Reagent Co., Ltd., China). Having been stirred for 30 min, the above solution was transferred into 70-mL stainless steel autoclave and maintained at 160 °C for several hours. Then, the reaction was stopped and cooled to room temperature. The precipitate was collected and rinsed with ethanol four times and dried at 60 °C for 12 h in a vacuum oven, and calcined at 500 °C for 2 h. The as-prepared sample was marked as Ag-nanowires@$TiO_2$ core-shell nanostructures (ANTNs).

In a typical procedure, 0.5 mL of 2 mg/mL ANTNs suspension aqueous, 0.25 mL of 10 mg/mL Hb PBS (0.1 M, pH 7.0), and 0.25 mL of Nafion (5 wt%) were kept ultrasonically dispersing for 30 min and then 4 μL of as-prepared mixture was cast onto a cleaned GCE surface to form uniform film electrode.

For comparison with Hb-ANTNs-Nafion/GC, the sample of $TiO_2$ nanowires with relative smooth surface (denoted as $TiO_2$ (s)) was synthesized and used for the fabrication of Hb-

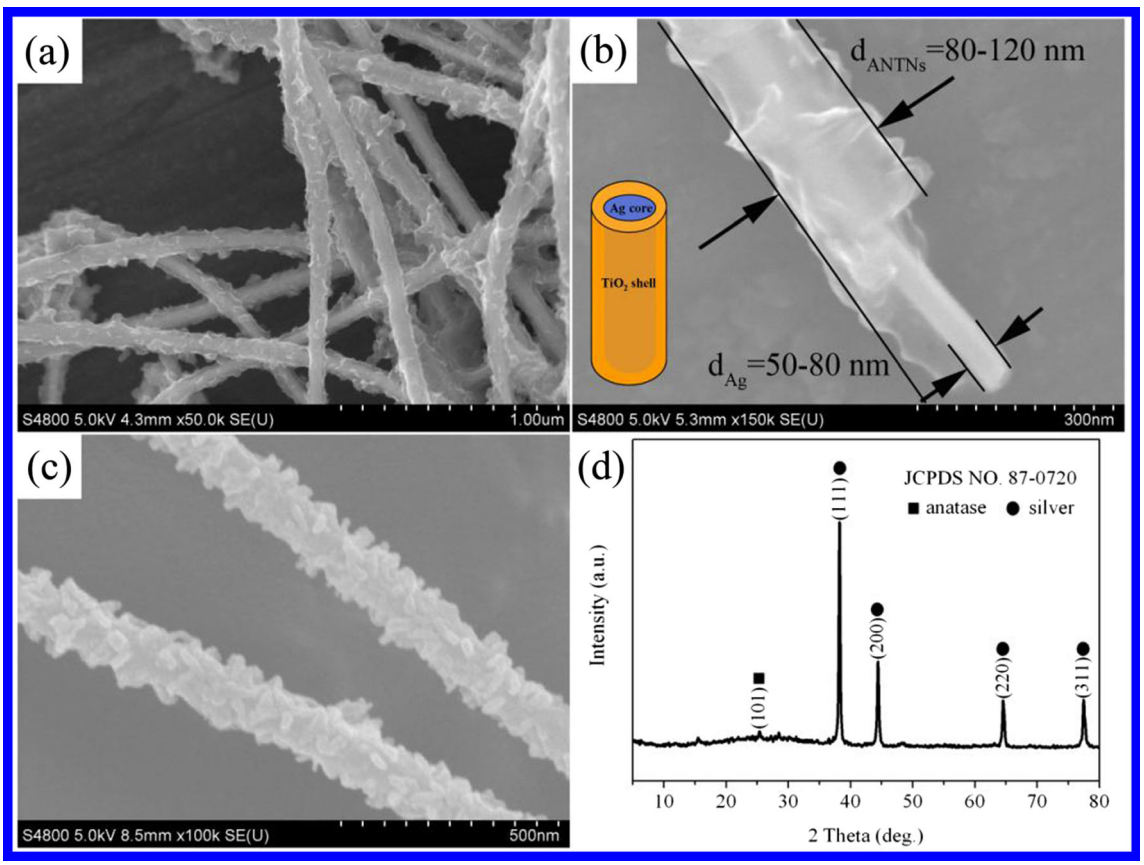


**Fig. 1** SEM images of the core-shell structures, before (**a**, **b**) and after calcined (**c**) higher images of ANTNs, and (**d**) XRD pattern of the ANTNs. The inset in **b** gives the schematic plot and their corresponding diameters of the as-prepared ANTNs core-shell structures

$TiO_2$(s)-Nafion/GC electrodes with similar procedures as described above. Figures S1 and S2 (Supporting Information) give the SEM images and XRD patterns of the solid $TiO_2$ (s) nanowires with an average diameter of about 100 nm.

*Characterization* The products were analyzed by X-ray diffraction (XRD, D/max-2200) using $CuK_\alpha$ radiation ($\lambda$= 0.154 nm). The morphology and characterization of the products were performed by field emission scanning electron microscopy (FE-SEM; Hitachi S-4800 & Hiroba EDX electron microscopy). The electrochemical properties of the ANTNs-based biosensor were performed at room temperature using a CHI 660 workstation (CH Instruments, Inc., China). A conventional three-electrode cell was used, including a glassy carbon electrode as the working electrode, an Ag/AgCl electrode as the reference electrode, and a platinum foil as the counter electrode.

## Results and discussion

Figure 1 exhibits the typical SEM images and the XRD pattern of ANTNs. Obviously seen from Fig. 1a, the well monodispersed and uniform precursors were composed of large quantities of one-dimensional nanostructures with the diameter of about 80–120 nm. As for the typical Ag@$TiO_2$ core-shell structures, the silver nanowires were encapsulated by a layer of amorphous $TiO_2$. Typically, the thickness of the $TiO_2$ shell was about 20–30 nm, and the diameter of the silver core was around 50–80 nm (Fig. 1b). Besides, the inset in b gives the schematic plot and their corresponding diameters of the as-prepared ANTNs core-shell structures. After calcination, amorphous $TiO_2$ shell became further crystalline to unique rod-like nanoparticles (Fig. 1c). Therefore, the ANTNs could possess a comparatively rough surface so as to enhance the immobilization of hemoglobin, and thus accelerating the

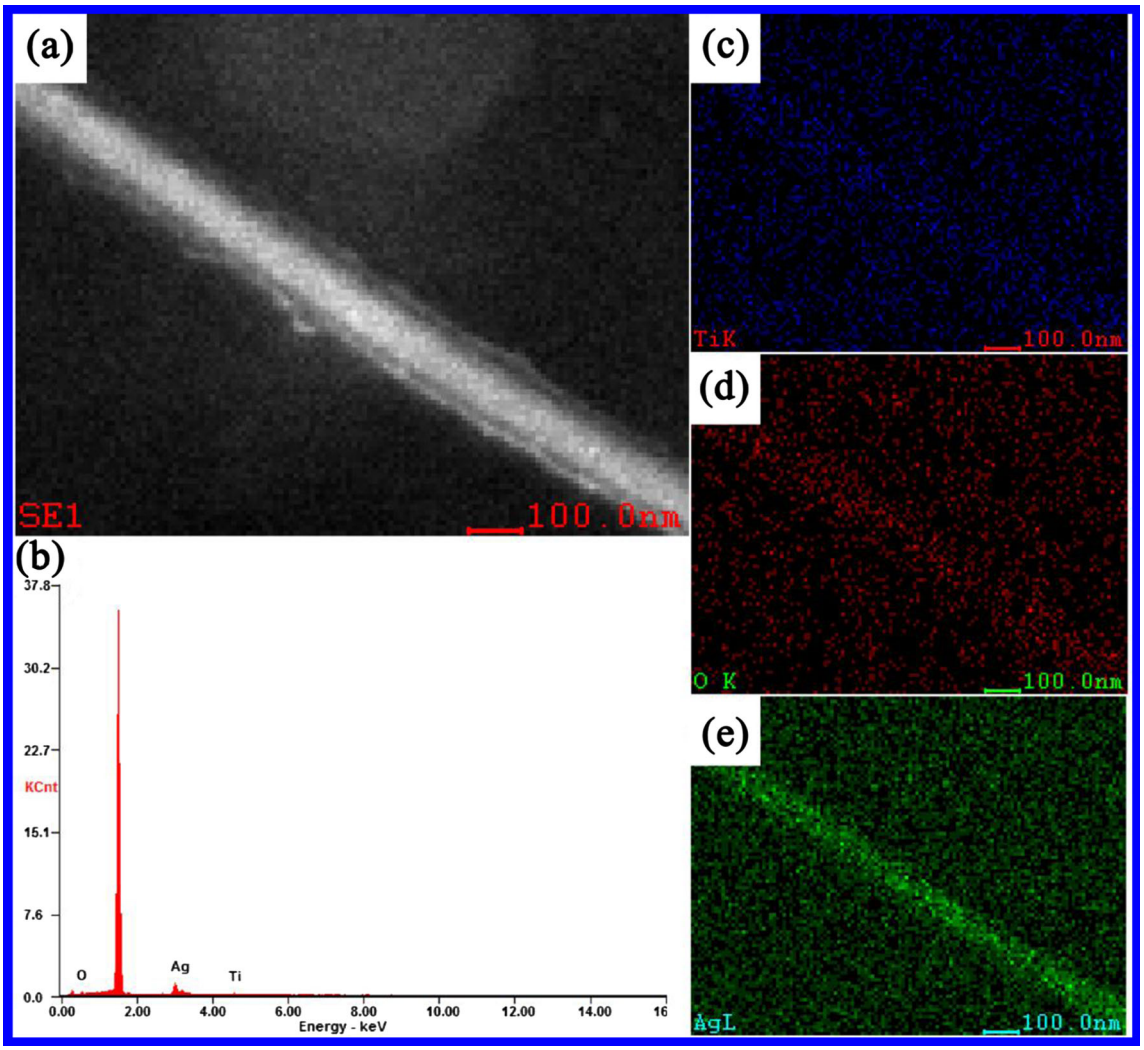


**Fig. 2** EDX and elemental mapping of the as-prepared ANTNs precursor, **a** SEM image of ANTNs precursor, **b** EDX spectroscopy of ANTNs precursor, and **c**–**e** correspond to the EDX elemental mapping images of Ti, O, and Ag, respectively

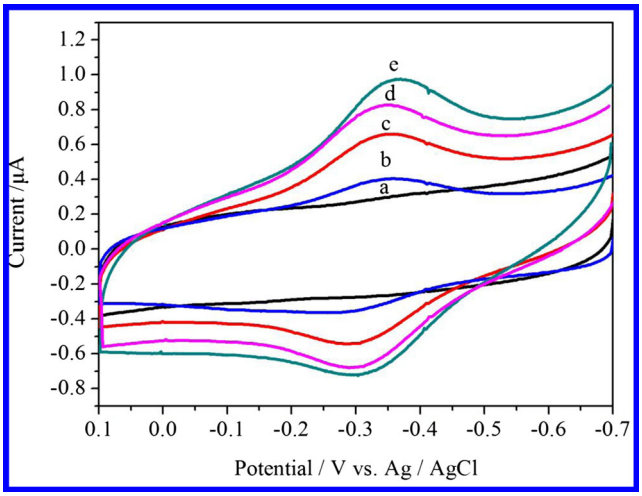


**Fig. 3** Cyclic voltammograms of different modified electrode in pH 7.0 PBS with scan rate of 0.1 V $s^{-1}$ **a** ANTNs-Nafion/GC, **b** Hb-Nafion/GC, **c** Hb-$TiO_2$(s)-Nafion/GC, **d** Hb-silver nanowires-Nafion/GC, and **e** Hb-ANTNs-Nafion/GC

electron transfer because of the silver nanowires existing in the unique one-dimensional Ag-nanowires@$TiO_2$ core-shell nanostructure. As shown in Fig. 1d, four strong and sharp peaks were observed, which were attributed to the diffraction of (111), (200), (220), and (311) planes of 3C-silver (JCPDS Card No. 87–0720), respectively [25]. Furthermore, one weak diffraction peak in the patterns was assigned to the diffraction of (101) plane of anatase $TiO_2$ (JCPDS Card No. 21–1272), which might be due to the low amount of $TiO_2$ shell [26].

Figure 2b is the corresponding energy dispersive X-ray spectroscopy of the sample of ANTNs precursor shown in Fig. 2a, which shows that the obtained one-dimensional microstructures with the diameter of about 80–120 nm are composed of the elements Ti, O, and Ag. Figure 2c–e corresponds to the EDX elemental mapping images of Ti, O, and Ag, which shows that the distribution of the Ti and O species on the surface of silver nanowires with the diameter of about 50–80 nm are homogeneous, and also confirms the formation of the unique Ag-nanowires@$TiO_2$ core-shell structures.

We also observed the FTIR spectra of (a) Hb and (b) Hb–AgNW@$TiO_2$-Nafion composite film (Supporting Information Fig. S3). The characteristic peaks at approximately 1,658 and 1,540 $cm^{-1}$ (curve a) could be ascribed to the FTIR spectra of $amide^{I}$ (1,700–600 $cm^{-1}$) and $amide^{II}$ (1,620–1,500 $cm^{-1}$) bands of native Hb, respectively, (curve a) [27, 28]. As shown in curve b, the spectra of Hb in the Nafion-ANTNs films were similar with that of curve a, suggesting that the ANTNs heterojunctions have good biocompatibility with Hb.

Figure 3 depicts typical cyclic voltammograms of different modified electrodes in 0.1 M pH 7.0 PBS. A pair of stable and well-defined redox peaks of Hb for the Hb($Fe^{III}$)/Hb($Fe^{II}$) redox couple transformation, which could be ascribed to the direct electron transfer between the Hb and the ANTNs-Nafion/GC electrode (Fig. 2d), is observed clearly. The formal potential $E^{0'}$($E^{0'} = (E_{p,a} + E_{p,c})/2$) of Hb was −0.345 V versus Ag/AgCl, characteristic of Hb($Fe^{III/II}$) redox couples. The potential difference $\Delta E_p$ between the anodic and cathodic peak potentials, which is directly related to the electron transfer rate, was about 50 mV. Such a small $\Delta E_p$ value revealed a fast and quasi-reversible electron-transfer process. The redox peaks observed at the Hb-Nafion/GC (Fig. 3b) were much smaller than that of Hb-ANTNs-Nafion/GC electrode, which may be attributed that the ANTNs could enhance the direct electron transfer of Hb by the synergetic effect with Nafion. Moreover, Nafion is a good proton-conducting polymer; the good conductivity of the ANTNs-Nafion composite contributes to the efficient electron transfer. Besides, the redox peaks of Hb-$TiO_2$-Nafion/GC were much smaller than that of Hb-ANTNs-Nafion/GC. The $\Delta E_p$ of Hb-$TiO_2$-Nafion/GC was 100 mV, which was larger than that of Hb-ANTNs-Nafion/GC (50 mV), indicating a slower electron transfer rate of Hb on Hb-$TiO_2$-Nafion/GC than on Hb-ANTNs-Nafion/GC. The

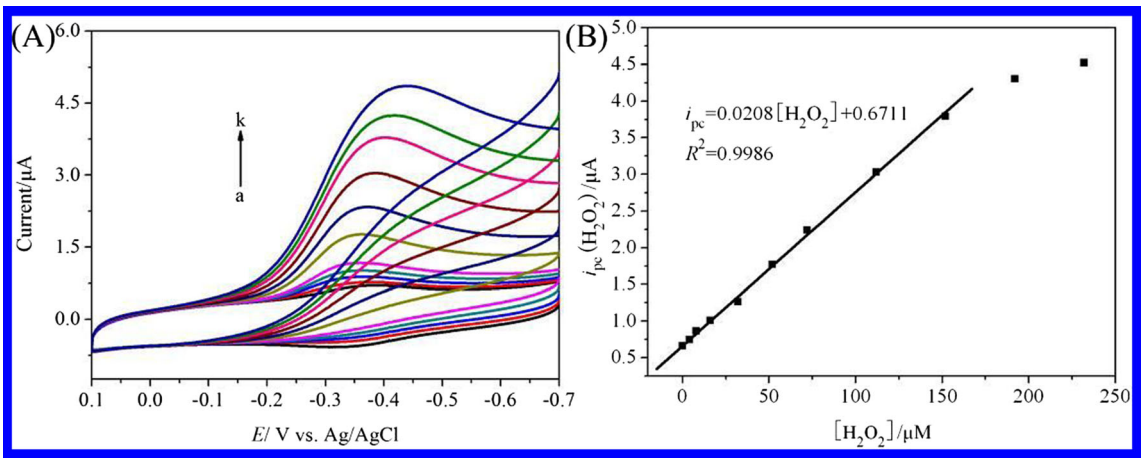


**Fig. 4** **a** Bioelectrocatalysis of the biosensor towards $H_2O_2$ in pH 7.0 PBS with scan rate 0.1 V $s^{-1}$, $H_2O_2$ concentrations (μM): *a* 0, *b* 4, *c* 8, *d* 16, *e* 32, *f* 52, *g* 72, *h* 112, *i* 152, *g* 192, and *k* 232. **b** The calibration curve of cathodic reduction current versus $H_2O_2$ concentration

redox peaks of Hb-silver nanowires-Nafion/GC was also smaller than that of Hb-ANTNs-Nafion/GC, which maybe due to the lower adsorption for Hb caused by the much smoother surface of silver species (Supporting Information Fig. S4). Therefore, the unique ANTNs core-shell structure could combine adsorption of $TiO_2$ shell with the conductivity of silver nanowires core so as to improve the electrochemical activities of Hb-ANTNs-Nafion/GC-based biosensor.

To further investigate the electrochemical characteristics of the Hb-ANTNs-Nafion/GC electrode surface, the dependence of the peak currents on the scan rate was systemically studied in the range of 0.1–0.8 V $s^{-1}$ (Supporting Information Fig. S5). With increasing scan rates, the cathodic and anodic peak currents of Hb both increase, while the cathodic and anodic peak potentials showed a small shift and the peak to peak separations became slightly enlarged (Fig. S5a). The cathodic and anodic peak currents increased linearly with scan rates from 0.1 to 0.8 V $s^{-1}$ (Fig. S5b), which revealed that the electron transfer between Hb and a GC electrode could be easily performed in the Hb-$TiO_2$-Nafion composite film and that a surface-controlled electrochemical process is involved. According to the Laviron method for a surface-controlled electrochemical system [29], the average electron transfer rate constant ($k_s$) of Hb immobilized on ANTNs-Nafion/GC was estimated to be about 4.7 $s^{-1}$, which is higher than the value reported for Hb immobilized on ZnO microspheres (3.2 $s^{-1}$) [27], suggesting a faster electron transfer process. This means that the Ag-nanowires@$TiO_2$ core-shell nanostructures accelerate the direct electron transfer of Hb.

The direct electrochemistry of Hb immobilized on the ANTNs-Nafion/GC electrode showed a strong dependence on the solution pH. Figure S5 shows the CVs of the Hb-ANTNs-Nafion/GC electrode in PBS with different pH values (Supporting Information Fig. S6). CVs with stable and well-defined peaks were observed in the pH range 6.0 to 8.0, but increasing pH caused a negative shift of both cathodic and anodic peak potentials. This attributed to the involvement of proton transfer in the Hb-Fe($^{III}$)/Hb-Fe($^{II}$) redox couple. The $E^{0'}$ value of Hb varied linearly in the pH range from 6.0 to 8.0, with a slope of −50.2 mV/pH. This value is very close to the theoretical value for transfer of one proton and one electron in a reversible reduction (−58 mV/pH at 25 °C) [12, 30].

Figure 4a reveals the bioelectrocatalytic activity of the enzyme electrode for the reduction of $H_2O_2$ at a rate of 0.1 V $s^{-1}$. A pair of reversible CV peaks appeared in the absence of $H_2O_2$ (curve a). Upon addition of $H_2O_2$ to the pH 7.5 PBS, the reduction peak current of immobilized Hb increased and the oxidation peak current decreased (curve b–k). These results indicated that the immobilized Hb on ANTNs-Nafion film maintained its electrocatalytic activity for the reduction of $H_2O_2$. Figure 4b revealed cathodic reduction currents at about −0.36 V increased linearly with the increasing $H_2O_2$ concentration. The linear range was from 4 to 152 μM ($R^2$=0.9986), depicting that the enzyme electrode had good bioelectrocatalytic activity for $H_2O_2$. Further increasing the $H_2O_2$ concentration resulted in a rise in the catalytic current up to a limiting value; such saturation behavior was characteristic of enzyme-based catalysis.

The long-term stability of the Hb-ANTNs-Nafion/GC electrode electrochemical sensor was investigated by examining its current response during storage in a refrigerator at 4 °C. The electrochemical sensor exhibited no obvious decrease in current response in the first week and maintained about 93 % of its initial value after 3 weeks. The reproducibility of the biosensor was investigated by determining 15 and 30 μM $H_2O_2$ in PBS (pH 7.0). The relative standard deviation (RSD) was 2.5 and 3.1 %, respectively, for four successive measurements, indicating the good reproducibility.

## Conclusions

We have constructed a simple but practical Hb-ANTNs-Nafion/GC-based biosensor and studied the electrochemical behavior of Hb with this modified GC electrode. Cyclic voltammetric results showed that $TiO_2$ shell could provide a microenvironment to immobilize Hb and silver core could further accelerate the direct electron transfer at the electrode surface. The as-prepared Hb-ANTNs-Nafion/GC-based biosensor can be used for the efficient entrapment of other redox active proteins and have wide potential applications in biosensors, biocatalysis, biomedical devices, etc.

**Acknowledgment** This work was financially supported by the National Science Foundation of China (51272147), the Academic Backbone Cultivation Program of Shaanxi University of Science & Technology (XSGP201203), and the Graduate Innovation Found of Shaanxi University of Science and Technology.

## References

1. Cui Y, Lieber C (2001) Science 291:851–853
2. Du JM, Zhang JL, Liu ZM, Han BX, Jiang T, Huang Y (2006) Langmuir 22:1307–1312
3. Hoffmann MR, Martin ST, Choi W, Bahnemann DW (1995) Chem Rev 95:69–96
4. Zhu YH, Cao HM, Tang LH, Yang XL, Li CZ (2009) Electrochim Acta 54:2823–2827
5. Yan K, Wang R, Zhang JD (2014) Biosens Bioelectron 53:301–304
6. Bao SJ, Li CM, Zang JF, Cui XQ, Qiao Y, Guo J (2008) Adv Funct Mater 18:591–599
7. Kim JB, Grate JW, Wang P (2006) Chem Eng Sci 61:1017–1026
8. Wang YF, Wu MY, Zhang WF (2008) Electrochim Acta 53:7863–7868
9. Zheng W, Zheng YF, Jin KW, Wang N (2008) Talanta 74:1414–1419
10. Liu S, Chen A (2005) Langmuir 21:8409–8413
11. Zhang L, Zhang Q, Lu XB, Li JH (2007) Biosens Bioelectron 23:102–106

12. Xie Q, Zhao YY, Chen X, Liu HM, Evans DG, Yang WS (2011) Biomaterials 32:6588–6594
13. Cozzoli PD, Comparelli R, Fanizza E, Curri ML, Agostiano A, Laub D (2004) J Am Chem Soc 126:3868–3879
14. Kamat PV, Hirakawa T (2005) J Am Chem Soc 127:3928–3934
15. Sun JY, Huang KJ, Zhao SF, Fan Y, Wu ZW (2011) Bioelectrochem 82:125–130
16. Huang KJ, Li J, Wu YY, Liu YM (2013) Bioelectrochem 90:18–23
17. Guo CX, Hu FP, Li CM, Shen PK (2008) Biosens Bioelectron 24: 819–824
18. Wang Y, Ma XL, Wen Y, Xing YY, Zhang ZR (2010) Biosens Bioelectron 25:2442–2446
19. Slamet XX, Nasution HW, Purnama E, Kosela S, Gunlazuardi J (2005) Catal Commun 6:313–319
20. Rupa AV, Manikandan D, Divakar D, Skvakumar T (2007) J Hazard Mater 147:906–913
21. Cao YW, Jin RC, Mirkin CA (2001) J Am Chem Soc 123:7961–7962
22. Yun HJ, Lee H, Kim ND, Yi J (2009) Electrochem Commun 11:363–366
23. Sun H, Choy TS, Zhu DR, Yam WC, Fung YS (2009) Biosens Bioelectron 24:1405–1410
24. Khan MM, Ansari SA, Amal MI, Lee J, Cho MH (2013) Nanoscale 5:4427–4435
25. Xiao J, Xie Y, Tang R, Chen M, Tian X (2001) Adv Mater 13:1887–1891
26. Cui YM, Liu L, Li B, Zhou XF, Xu NP (2010) J Phys Chem C 114: 2434–2439
27. Lu XB, Zhang HJ, Ni YW, Zhang Q, Chen JP (2008) Biosens Bioelectron 24:93–98
28. Feng XM, Cheng YF, Ye C, Ye JS, Peng JY, Hu JQ (2012) Mater Lett 79:205–208
29. Laviron E (1979) J Electroanal Chem 101:19–28
30. Wu FH, Xu JJ, Tian Y, Hu ZC, Wang LW, Xian YZ, Jin LT (2008) Biosens Bioelectron 24:198–203